

Dielectric and Microstructure Studies of Lead Magnesium Niobate Prepared by Partial Oxalate Route

Surya Mohan Gupta & Ajit R. Kulkarni

Department of Metallurgical Engineering and Materials Science, Indian Institute of Technology, Powai, Bombay 400 076, India

(Received 27 January 1995; revised version received 12 June 1995; accepted 28 June 1995)

Abstract

Lead magnesium niobate (PMN) has been prepared using the partial oxalate method without addition of excess PbO and sintering at four different temperatures, 900, 1000, 1100 and 1200°C. Increase in the sintering temperature resulted in increased dielectric constant which is attributed to an increase in the grain size. Here we report an unusually high dielectric constant (24 000 at -16°C , 1 kHz) observed in PMN sintered at 1200°C [PMN(1200)]. The room temperature dielectric constant and dissipation factor at 1 kHz is ~ 15000 and 0.0025, respectively, for PMN(1200). These values are superior to the reported values. A detailed and systematic study on phase, physical and dielectric properties and microstructure has been carried out. Grain size appears to be a dominant factor in controlling dielectric constant rather than the pyrochlore phase, as claimed earlier.

1 Introduction

Lead magnesium niobate (PMN) has been widely studied in recent years because of its attractive properties, such as: (i) high dielectric constant of 18 000 and 20 000 at T_c for poly- and single crystals,¹ respectively; (ii) low firing temperature (900°C) that allows the use of low cost Ag:Pd electrodes; and (iii) a very broad dielectric constant against temperature curve. The main hindrance in the commercial exploitation of this material arises from processing difficulties. It has been recognized and widely accepted that the reproducibility is diminished by the stable pyrochlore phase that forms at low temperature (700°C). It has been reported that a very small amount of this phase reduces the dielectric constant remarkably.

A number of methods have been suggested to eliminate or minimize the pyrochlore phase. These

involve modification of solid state or wet chemical methods, but most of them leave 3–5% pyrochlore phase in the sintered product.^{2–10} Authors have recently compiled advantages and disadvantages of these methods.^{11,12} Among all the methods reported so far, the Columbite method has proved to be one of the most successful. It gives nearly single-phase PMN because of the non-availability of free niobium oxide and lead oxide to form the pyrochlore phase. However, inhomogeneous mixing in the Columbite precursor leads to formation of pyrochlore phase and subsequent deterioration of dielectric properties. To improve the mixing and the reactivity of ceramic powders the partial oxalate route was adopted successfully for the fabrication of perovskite PMN.¹³

All methods have claimed perovskite phase formation from X-ray diffraction studies but dielectric behaviour varies considerably from method to method, and under such conditions microstructure examination of the ceramic proves useful. Shrout *et al.*¹⁴ using transmission electron microscopy (TEM) observed that each grain is covered with a very thin layer of second phase of the order of 1–2 nm. This phase is also found at triple point boundaries along with impurities derived from the raw materials or introduced during processing, and was believed to be PbO. Wang and Schulze¹⁵ examined the role of a PbO grain boundary phase on the dielectric properties of PMN. The PbO grain boundary layer for stoichiometric PMN was calculated to be 1.2 nm thick when the sample was sintered at 1200°C for 1 h.

The objective of this work was to study the effect of change in the PbO grain boundary layer on the dielectric properties of PMN. A chemical route with high purity starting reagents may lead to a product in which only unreacted or excess PbO will be present at the grain boundaries. A systematic and detailed study of phase analysis, physical properties, dielectric properties and microstructure has been carried out to reveal the

effect of the PbO grain boundary layer on the dielectric properties of PMN.

2 Experimental Procedure

Starting powders niobium oxide (Nb_2O_5) (special pure grade, Aldrich, USA), magnesium carbonate (MgCO_3) and lead nitrate ($\text{Pb}(\text{NO}_3)_2$) (reagent grade, BDH, UK) were used as-received. The lead solution was prepared by dissolving $\text{Pb}(\text{NO}_3)_2$ in double-distilled water. The flow diagram of the partial oxalate route is shown in Fig. 1. The Columbite precursor was prepared by mixing MgCO_3 and Nb_2O_5 in methanol for 1 h using an automated agate mortar and pestle (RETSCH Mortar Grinder, Type RMO, Germany) and, after drying, was fired at 1100°C for 4 h. The procedure was repeated twice to ensure complete reaction. The formation of single-phase magnesium niobate was confirmed by X-ray diffraction (XRD). The precursor was sprinkled in oxalic acid solution, stirred for 1 h and then lead nitrate solution was added dropwise. In the reaction that follows lead nitrate precipitates as lead oxalate and it was assumed to coat¹⁶ the calcined powders giving a homogeneous mixture. These precipitates were washed several times with distilled water. The powder was presintered at 800°C . Presintered powder was crushed and mixed for 1 h in methanol using automated agate mortar and pestle. The mixed powder was pressed as discs (15 mm diameter, 2–3 mm thick) and sintered at 900, 1000, 1100 and 1200°C for 2 h in a closed alumina crucible at a rate of 3°C min^{-1} . It may be mentioned here that the pellets were buried in MgO powder and fired in a closed alumina crucible to minimize the lead oxide loss from the pellets. The phase analysis of the presintered and sintered ceramic was carried out using XRD (JEOL DL 5400, Japan) using Cu $K\alpha$ radiation of wavelength 1.5406 \AA .

For dielectric measurements, the sintered discs were polished on different grades of emery paper. Electrical contacts on the parallel surfaces were made by gold sputtering (Edward 360, UK). In addition the gold layer was covered with room temperature curable silver paint (Eltech, Bangalore, India) to improve the contacts. Dielectric properties were measured with an impedance gain phase analyser (Schlumberger, SI 1260, UK) at four different frequencies (0.1, 1, 10 and 50 kHz) with $1 V_{\text{rms}}$, during cooling over a range of temperatures (-30 to $+80^\circ\text{C}$). The temperature was controlled to $\pm 1^\circ\text{C}$. Microstructure analysis was performed by scanning electron microscopy (SEM) (Jeol JSM 6400, Japan) on the fractured surface.

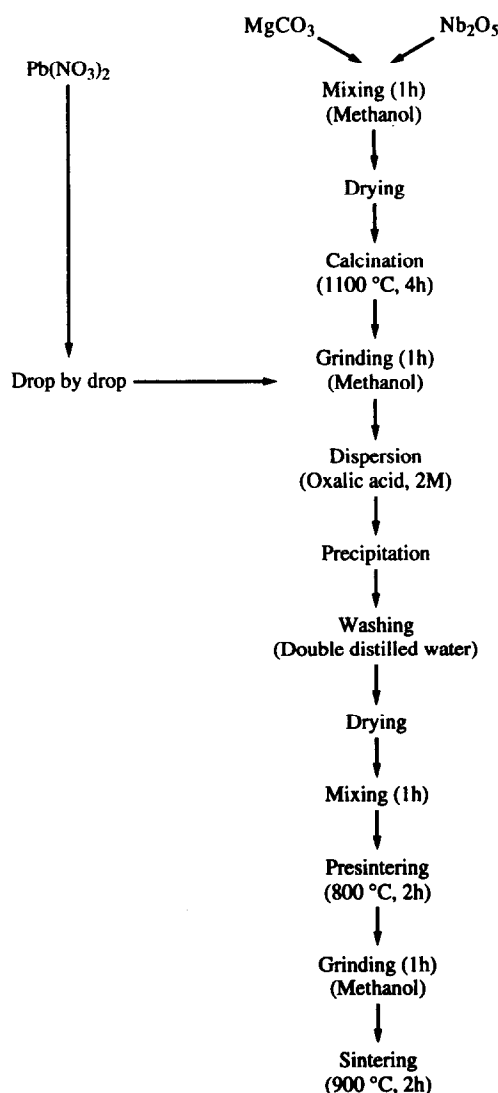
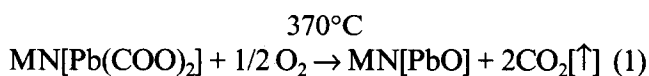


Fig. 1. Flow diagram of partial oxalate route for PMN preparation.

3 Results and Discussion

Differential thermal analysis (DTA) and thermal gravimetry analysis (TGA) of the PMN precursor, i.e. lead oxalate-coated magnesium niobate, are shown in Fig. 2. This study reveals that at 370°C , lead oxalate decomposes to lead oxide:



Here, MN stands for magnesium niobate. TGA shows a sharp weight loss at 370°C . The calculated weight loss agrees with the weight loss from reaction (1). Before proceeding to phase analysis, it may be mentioned that excess PbO was not added at any stage during fabrication, as it may increase the thickness of the PbO grain boundary layer around each grain. Most methods reported so far, however, emphasize the addition of excess PbO to minimize pyrochlore phase formation. This appears to be a major advantage over all other methods.

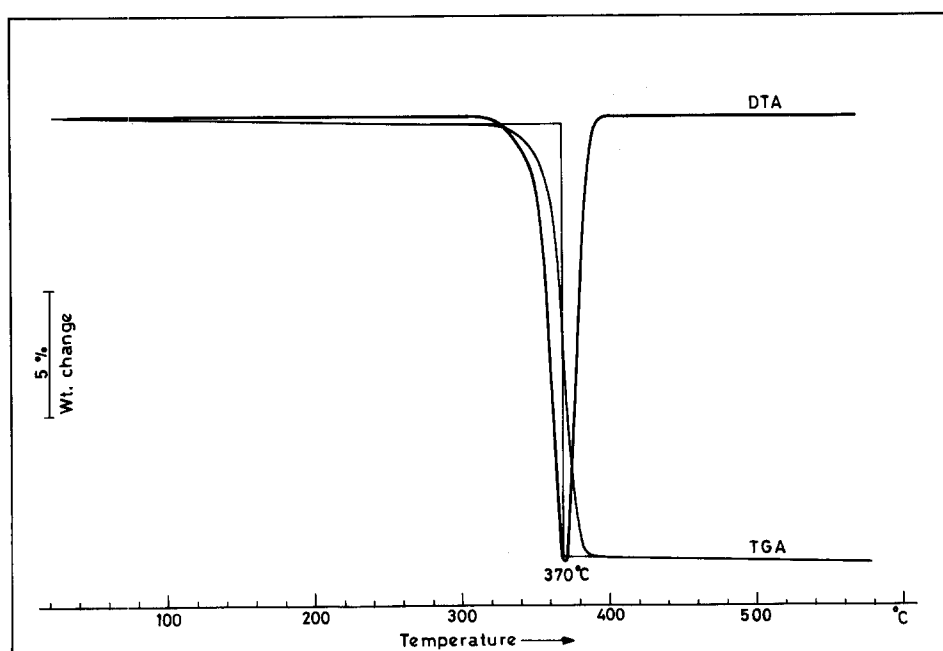
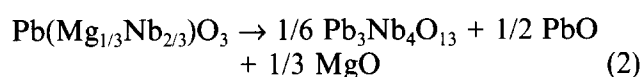


Fig. 2. Differential thermal analysis (DTA) and thermal gravimetric analysis (TGA) of uncalcined powder.

One important step in this process is to avoid lead oxide loss during firing. The processes that lead to PbO loss during firing induce an increase in the amount of pyrochlore phase, as is evident from the following reverse reaction:¹²



It may be mentioned that factors such as excess MgO and Nb₂O₅, mixing time, presinter temperature, etc., which are known to influence pyrochlore phase formation, were optimized while preparing PMN by the partial oxalate method.^{11,12}

3.1 Phase analysis

In general, the difficulty in sintering lead-containing materials is mainly attributed to the loss of lead oxide. Therefore, all the pellets were sintered in a closed crucible. The pellets were weighed before and after firing. This showed a 0.8 and 1.5% weight loss in PMN(900) and PMN(1000) samples, respectively, but nearly 6 and 9% weight loss was recorded for the PMN(1100) and PMN(1200) samples. (Numbers in bracket represent the sintering temperature of that sample.) The weight loss in the pellets is due to lead oxide loss only

because of the high volatility of lead oxide. The presintered powders and sintered pellets were analysed for the phases present XRD. The XRD pattern of the sintered samples as a function of sintering temperature is shown in Fig. 3. The recorded spectra agree well with the JCPDS values and confirm the formation of PMN. The amount of pyrochlore phase present in each sample is calculated from the relative intensities of the major X-ray reflection for the pyrochlore and the perovskite phase as reported in the literature:²

$$\text{Pyrochlore phase} = \frac{I_{\text{pyro}}}{I_{\text{pyro}} + I_{\text{PMN}}} \times 100 \quad (3)$$

where I_{pyro} refers to the (222) pyrochlore peak and I_{PMN} refers to the (110) perovskite peak. The percentage of perovskite phase and pyrochlore phase present in the sintered samples along with sample codes, physical properties and dielectric properties are given in Table 1.

It may be noticed that sintered specimens [Figs 3(b)–(e)] show nearly the same percentage of perovskite phase as compared to the presintered powders (PMN[P], Fig. 3(a)). No pyrochlore phase peak (222) was found in the PMN(900) and

Table 1. Phase analysis, physical and dielectric properties for PMN prepared by partial oxalate route at four different sintering temperatures

Sample No.	Samples	Phase analysis		Physical properties		Dielectric properties (1 kHz)		
		Perovskite (%)	Pyrochlore (%)	Density (g cm ⁻³)	Porosity	K _{max}	Tanδ	T _c (°C)
1	PMN(900)	100.0%	0.0%	4.78	41.28%	4000	0.019	-5
2	PMN(1000)	100.0%	0.0%	5.31	34.8%	8000	0.027	-7
3	PMN(1100)	98.0%	2.0%	5.42	32.78%	12000	0.037	-11
4	PMN(1200)	96.0%	4.0%	7.21	06.88%	24000	0.046	-16

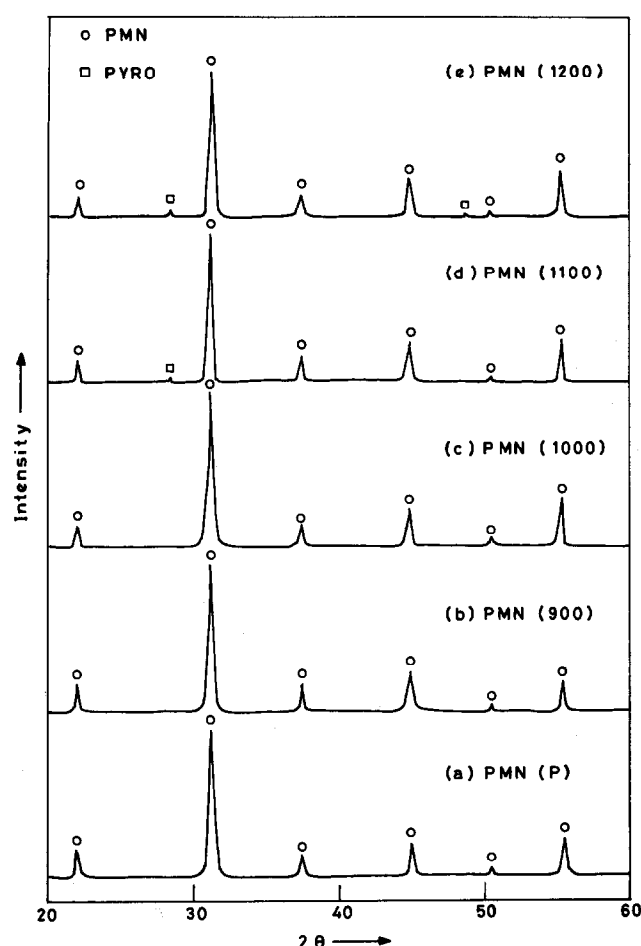


Fig. 3. X-ray diffraction pattern of PMN powder prepared by partial oxalate route: (a) presintered at 800°C, PMN(P); (b) sintered at 900°C, PMN(900); (c) sintered at 1000°C, PMN(1000); (d) sintered at 1100°C, PMN(1100); (e) sintered at 1200°C, PMN(1200). The material was soaked for 2 h at each sintering temperature.

PMN(1000) samples. However, it increases to 4% in the PMN(1200) sample, which is due to a fair amount of lead oxide loss during sintering.

3.2 Dielectric properties

The temperature dependence of the dielectric constant and dissipation factor at 1 kHz as a function of sintering temperature is shown in Figs 4(a) and (b). All the specimens show a broad maxima for the dielectric constant and negligible dissipation factor (0.0025) at room temperature. The dissipation factor increases to ~0.046 at the Curie temperature (T_c). The dielectric constant (K_{max}) and loss maxima shift towards a higher temperature (T_c) with increasing frequency, exhibiting typical relaxor behaviour. The maxima in the dielectric constant versus temperature plots increases remarkably with increase in the sintering temperature. The maximum dielectric constant of PMN at 1 kHz increases from 4000 to 24000 as the sintering temperature increases from 900 to 1200°C.

Two interesting features in this study are as follows. Firstly, the sample containing a small

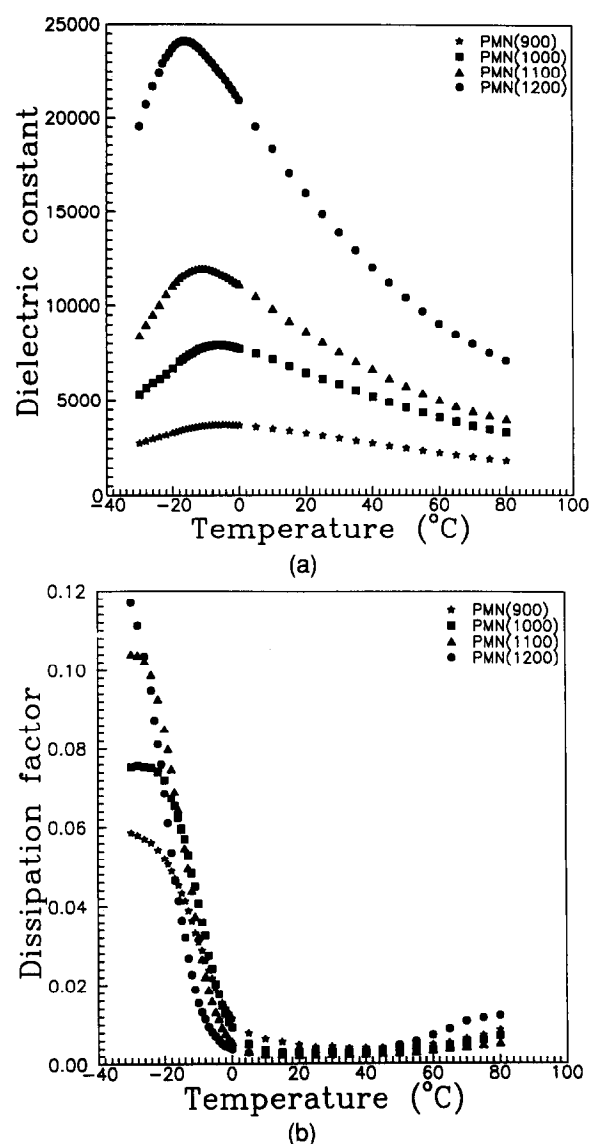


Fig. 4. Comparison of (a) dielectric constant (1 kHz) and (b) dissipation factor (1 kHz) versus temperature at different sintering temperatures.

amount of pyrochlore phase [0–2%, Figs 3(b)–(d)] shows a low dielectric constant (~4000–12000) which is contradictory to that in the work of ShROUT and Swartz¹⁷ but reinforces the work of Jie Chen *et al.*¹⁸ The latter found purity of the starting reagents more influential than the pyrochlore phase in controlling the dielectric properties of the materials.

The second feature is the dielectric constant (K_{max}) and dissipation factor behaviour of PMN(1200) shown in Figs 5(a) and (b). The sample shows all the characteristics of a relaxor material but with an exceptionally high dielectric constant of nearly 24000 at 1 kHz. This value is much higher than the highest reported values (~20000) for polycrystalline PMN.

It may be noted from Table 1 that the density of PMN(900) is very low compared to other samples but it shows all the characteristics of a relaxor material, which is generally difficult to achieve at

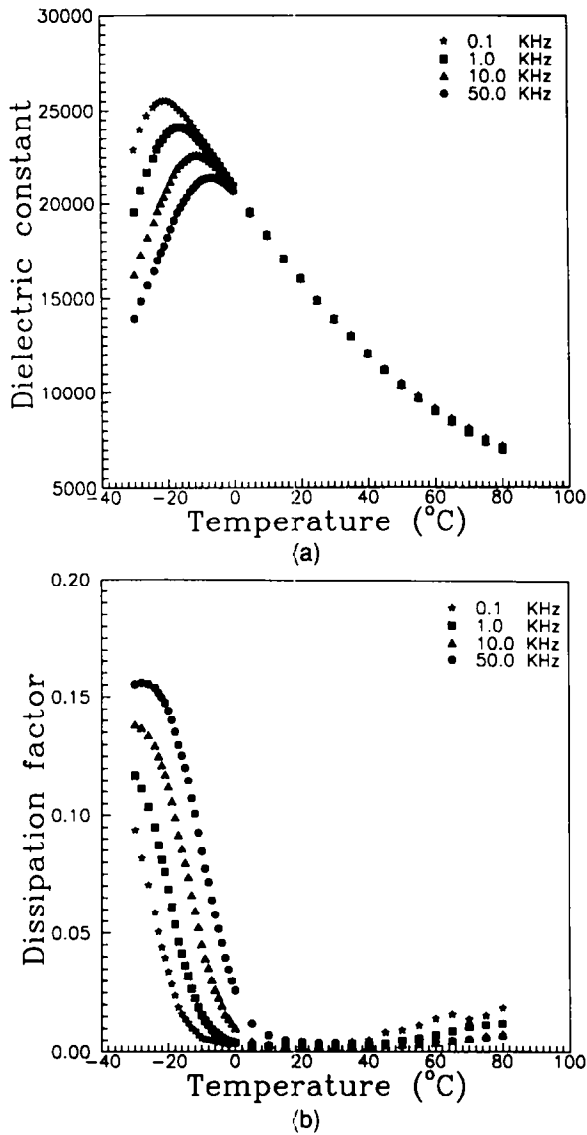


Fig. 5. Dielectric constant (a) and dissipation factor (b) versus temperature for PMN(1200) (stoichiometric composition, calcined at 800°C, sintered at 1200°C).

lower sintering temperatures. It is known that dielectric constant depends upon (i) phases present, (ii) density/porosity of the sample and (iii) grain size. To comment on the grain size effect, the dielectric constant values should first be corrected for porosity and the second phase present. The density and porosity of the compacts are determined using Archimedes' principle¹⁹ and are reported in Table 1. The dielectric constant (K_{\max}) is corrected for porosity of the samples using Rushman and Strivens' equation²⁰ which explains the effect of dispersed porosity (dielectric constant = 1) upon the dielectric constant of pure barium titanate. This equation has been widely used for correcting the porosity effect on the dielectric constant in ceramics.

$$K_{\text{corrected}} = \frac{K_{\text{observed}} \times (2 + V_2)}{2(1 - V_2)} \quad (4)$$

where V_2 is the volume fraction of porosity in the sample. The above equation was experimentally verified up to ~35% porosity ($V_2 = 0.35$). The samples containing more than this porosity has been corrected using Wiener's equation:²⁰

$$(K_{\text{PMN}} - K_S) \times (K_{\text{PORE}} + 2 K_{\text{PMN}}) = (K_{\text{PMN}} - K_{\text{PORE}}) \times V_2 \quad (5)$$

where K_{PMN} , K_{PORE} and K_S are the dielectric constant of the pure PMN, pore and sample, respectively. The observed and corrected dielectric constant (K_{\max}) values are reported in Table 2. The corrected value of dielectric constant (K_{\max}) shows a monotonic increase as the grain size increases. Similar dielectric grain size dependency in PMN and other lead-based relaxors has been observed.^{14,21} This dielectric dependency was explained by considering (i) microdipole-dipole co-operative interaction between superparaelectric regions²² and (ii) a low polarizable phase boundary. According to Viehland *et al.*²² the microdipole-dipole co-operative interaction accounts for the dispersive response of relaxor behaviour, and it maximizes near T_c to ~10–20 nm. Dielectric values of PMN as a function of grain are determined by following expression:

$$\ln K_{\text{PMN}} = V_{\text{Shell}} \ln K_{\text{Shell}} + V_{\text{Core}} \ln K_{\text{Core}} \quad (6)$$

where V_{Shell} and K_{Shell} and V_{Core} and K_{Core} are the volume and dielectric constants of the inactive 'shell' and core regions, respectively. The K_{Shell} value of ~300 was selected,²³ being of the order of an incipient ferroelectric and as the value found for PMN at cryogenic temperatures (~1 K) where domain effects would be frozen-out. Viehland *et al.*²² suggested a microdipole-dipole co-operative interaction between superparaelectric regions which enhances K and accounts for the dispersive response. This inactive or coherence length maximizes near T_c of the order of 10–20 nm. Inserting values of $K_{\text{Core}} = 20000$, the K_{\max} value of single crystal PMN, $K_{\text{Shell}} \sim 300$ and an inactive shell region of the order of 15 nm in eqn (6), the dielectric constant of PMN was determined as a function of size, where the core region is assumed to be the grain size. The dielectric constant of PMN as a function of grain size is presented in Table 2. It may be noted that the dielectric constant values derived from the logarithmic mixing rule [eqn (6)] show no agreement to the $K_{\text{Corrected}}$ values. It seems that the dielectric constant value of K_{Shell} and the thickness of the layer does not coincide with the second phase present around the grain in the present study.

Wang and Schulze¹⁵ also found that the dielectric constant decreases with the addition of excess

Table 2. Density correction on dielectric constant and average grain size for PMN prepared at four different sintering temperatures

Sample No.	Samples	K_{observed} (1 kHz)	$K_{\text{corrected}}^*$ (1 kHz)	Grain size (μm)	K_{PMN}^\dagger (1 kHz)	D_{gb} (nm)
1	PMN(900)	4000	8200 [‡]	~ 0.5	17697	0.72
2	PMN(1000)	8000	14300	~ 1.0	18796	0.39
3	PMN(1100)	12000	20800	~ 1.5	19185	<0.01
4	PMN(1200)	24000	26700	~ 3.0	19563	—

$$*K_{\text{corrected}} = \frac{K_{\text{observed}} \times (2 + V_2)}{2(1 - V_2)}$$

$$^\dagger \ln K_{\text{PMN}} = V_{\text{Shell}} \ln K_{\text{Shell}} + V_{\text{Core}} \ln K_{\text{Core}}$$

$$^\ddagger (K_{\text{PMN}} - K_s) \times (K_{\text{PORE}} + 2 K_{\text{PMN}}) = (K_{\text{PMN}} - K_{\text{PORE}}) \times V_2$$

PbO introduced during processing and explained the dependence according to a series mixing theory used for diphasic systems. This theory uses the following equation:

$$\frac{D}{K_s} = \frac{D_g}{K_g} + \frac{D_{\text{gb}}}{K_{\text{gb}}} \quad (7)$$

where K_s is the dielectric constant of the sample, K_g the dielectric constant of the perovskite PMN grain, K_{gb} the dielectric constant of the PbO solid solution in the grain boundary, D the thickness of the sample, D_g the thickness of the PMN grains and D_{gb} the thickness of the PbO grain boundary layers. Hilton²⁴ observed the presence of a very thin layer of second phase of the order of 1–2 nm located around each grain, using TEM, believed to be PbO-based regardless of process conditions. Shrout *et al.*¹⁴ postulated that along the grain boundaries amorphous PbO phase exists, which may be the reason for the reduction of the dielectric constant when grain size is small. Thus, the dielectric constant of the grain boundary is taken as the dielectric constant of PbO in eqn (7). The grain boundary in PMN is very thin. Therefore, D is approximately equal to D_g and eqn (7) reduces to:

$$\frac{1}{K_s} = \frac{1}{K_g} + \frac{1}{RK_{\text{gb}}} \quad (8)$$

where $R = D_g/D_{\text{gb}}$, i.e. the thickness ratio of the grain to the grain boundary layer. In the present study K_g (dielectric constant of the grain) is very much higher than K_{gb} (dielectric constant of the PbO in the grain boundary). The K_{gb} for PbO is 20 and not temperature dependent, whereas K_s is taken as $K_{\text{corrected}}$ and K_g is 20000, and these values are at T_c for the sample prepared and a single crystal of PMN, respectively.

Equation (8) has been used to calculate the thickness of the grain boundary layer. The thickness of the PbO grain boundary layer for each sample is calculated and presented in Table 2. Wang and Swartz¹⁵ compared the K_{max} of 13700

at 1 kHz with 20000, using the grain size of 2.1 μm for stoichiometric PMN, and the PbO grain boundary layer was calculated to be 1.2 nm thick when the sample was sintered at 1200°C for 1 h. It may be noted that the thickness reduces (0.72 to <0.1 nm) with increase in the sintering temperature (from 900 to 1100°C) or grain size (0.5 to 1.5 μm). The thickness of the PbO grain boundary layer could not be calculated for the PMN(1200) sample because the dielectric constant value is greater than the dielectric constant value of a single crystal. The reason for this unusual value has been explained²⁵ using X-ray photoelectron spectroscopy (XPS) studies on these samples. It has been found that the Pb atom is in two oxidation states (e.g. Pb^{2+} and Pb^{4+}) instead of one Pb^{2+} oxidation state. This dual oxidation state of Pb leads to an increased dipole moment and hence the high dielectric constant.

Shrout *et al.*¹⁴ observed drastically different values of K_{max} in PMN-PT (where PT = PbTiO_3) samples of similar grain sizes. These samples were kept underneath coarse zirconate sand and fired at different sintering temperatures. These different values have been explained on the basis of the amount of the amorphous PbO grain boundary phase present. It has been proposed that zirconate sand promotes amorphous PbO loss during sintering. Similarly, samples were kept underneath MgO powder in the present study and fired. It may be concluded that MgO powder promotes the amorphous PbO loss at low sintering temperature (up to 1100°C). This may be the reason for the very low density of the PMN(900), PMN(1000) and PMN(1100) samples.

The transition temperature shifts to the lower side with increase in the grain size. A similar transition temperature shift has also been observed in PMN and PMN-PT systems by other workers.^{14,17,21} No explanation as to why T_c shifts with grain size can be given at this time. The grain size variation with sintering temperature is described below with the results on microstructure.

3.3 Microstructure

The scanning electron micrographs of a fracture surface of the compact obtained on firing at 900, 1000, 1100 and 1200°C are shown in Figs 6(a)–(d). These micrographs demonstrate the effect of sintering temperature. All samples show 100% intergranular fracture. In Fig. 6(a), i.e. SEM(900), there are grains of an average grain size $\sim 0.5 \mu\text{m}$ with high porosity. It can be noticed in Figs 6(a)–(d) that porosity decreases and grain size increases with increase in the sintering temperature, which is generally observed. A gradual development of grain structure is clearly observed in other samples [PMN(1000) and PMN(1200)] which show well-developed grain morphology. It may be noticed that the magnification and voltage is kept the same while studying the microstructure of these samples. Careful observation of the microstructure reveals that grain size increases with increase in the sintering temperature. It may be noted that there is no secondary phase present in these samples. The average grain size increases from 0.5 to $3.0 \mu\text{m}$ with increase in the sintering temperature. On comparing the grain size and dielectric constant ($K_{\text{corrected}}$) in Table 2 it may be

concluded that the dielectric constant value increases remarkably with increase in grain size.

The most important result of this investigation was the apparent grain size dependence on the dielectric constant of PMN ceramics. The grain size, dependency was caused by the influence of the grain boundary volume, as suggested by Swartz *et al.*¹⁷ As the grain size increases, the number of boundaries in series with the grains decreases and the large permittivity of the PMN grains becomes less affected by the permittivity of the grain boundary. Present results suggest that the pyrochlore phase is not the only major detrimental factor to the dielectric behaviour of PMN.

4 Conclusions

Single-phase PMN with good dielectric properties has been prepared successfully by the partial oxalate method. Thermal analysis shows that lead oxalate decomposes at 370°C to form lead oxide. Phase analysis shows the formation of a single phase at low sintering temperature whereas the presence of nearly 4% pyrochlore phase in

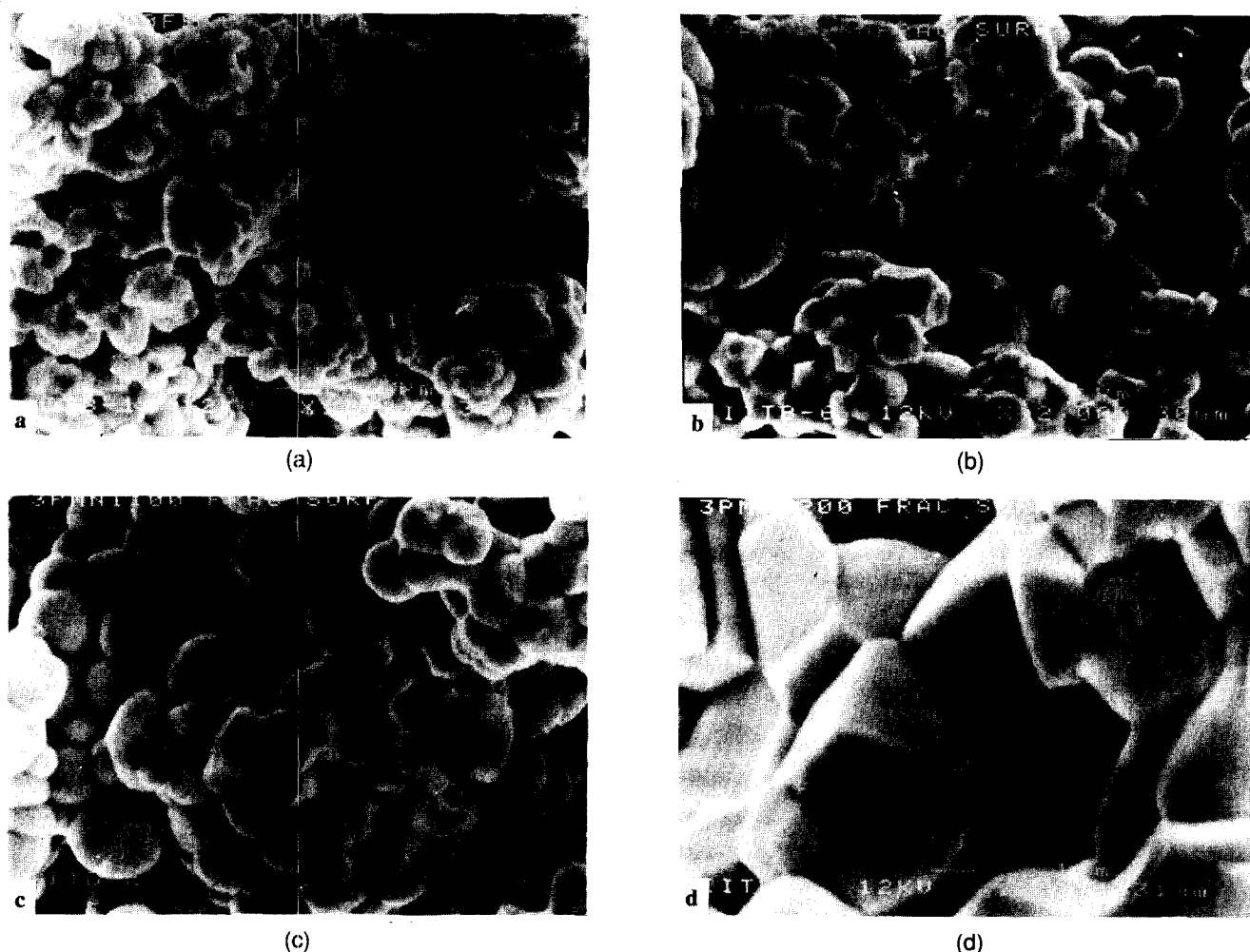


Fig. 6. Microstructure of sample: (a) sintered at 900°C, PMN(900); (b) sintered at 1000°C, PMN(1000); (c) sintered at 1100°C, PMN(1100); (d) sintered at 1200°C, PMN(1200) (calcined at 800°C for 2 h).

PMN(1200) sample is attributed to lead oxide loss. Dielectric constant values after porosity correction increase with increase in sintering temperature or grain size, which is due to the decrease in the thickness of the PbO grain boundary layer. All the sintered samples show good relaxor behaviour, including PMN(900), which shows a very low dielectric constant value because of large porosity. The dielectric properties reveal that the pyrochlore phase is not the main detrimental factor to the dielectric properties. Microstructure analysis reveals that grain size also controls the dielectric properties and in this case appears to be more dominant than the pyrochlore phase.

Acknowledgements

The authors thank their colleagues for kind support and helpful suggestions. They are particularly grateful to Dr J. Bellare of the Chemical Engineering Department for providing the SEM facility.

References

1. Bokov, V. A. & Myl'nikova, I. E., Electrical and optical properties of single crystals of ferroelectrics with a diffused phase transition. *Sov. Phys. Solid State*, **3**(3) (1961) 613–23.
2. Swartz, S. L. & Shrout, T. R., Fabrication of perovskite lead magnesium niobate. *Mater. Res. Bull.*, **17** (1982) 1245–50.
3. Lejeune, M. & Boilot, J. P., Optimisation of dielectric properties of lead magnesium niobate ceramics. *Am. Ceram. Soc. Bull.*, **64**(4) (1984) 679–82.
4. Lejeune, M. & Boilot, J. P., Low firing dielectric based on lead magnesium niobate. *Mater. Res. Bull.*, **20** (1985) 493–9.
5. Guha, J. P. & Anderson, H. U., Preparation of perovskite $\text{Pb}(\text{Mg}_{1/3}\text{Nb}_{2/3})\text{O}_3$ using $\text{Pb}_3\text{Nb}_2\text{O}_8$ and MgO . *J. Am. Ceram. Soc.*, **69**(11) (1986) C-287–8.
6. Chaput, F., Boilot, J. P., Lejeune, M., Papiernik, R. & Pfaizrag, L. G., Low temperature route to lead magnesium niobate. *J. Am. Ceram. Soc.*, **72**(8) (1989) 1355–7.
7. Katayama, K., Abe, M. & Akiba, T., Preparation of $\text{Pb}(\text{Mg}_{1/3}\text{Nb}_{2/3})\text{O}_3$ powder by molten salt method. *Ceram. Intl*, **15** (1989) 289–95.
8. Choy, J. H., Yoo, J. S., Kang, S. Gu., Hong, S.T. & Kim, D. G., Ultrafine $\text{Pb}(\text{Mg}_{1/3}\text{Nb}_{2/3})\text{O}_3$ (PMN) powder synthesised from metal citrate gel by thermal shock method. *Mater. Res. Bull.*, **25** (1990) 283–91.
9. Shrout, T. R., Papet, P., Kim, S. & Lee, Gye-Song, Conventionally prepared submicrometer lead-based perovskite powders by reactive calcination. *J. Am. Ceram. Soc.*, **73**(7) (1990) 1862–7.
10. Watanabe, A., Haneda, H., Mosiyoshi, Y., Shirasaki, S., Kuramoto, S. & Yamamura, A., Preparation of lead magnesium niobate by a coprecipitation method. *J. Mater. Sci.*, **27** (1992) 1245–9.
11. Gupta, S. M. & Kulkarni, A. R., Synthesis and dielectric properties of lead magnesium niobate – a review. *Mater. Chem. Phys. J.*, **39** (1994) 98–109.
12. Gupta, S. M. & Kulkarni, A. R., Synthesis of perovskite lead magnesium niobate using partial oxalate method. *Mater. Res. Bull.*, **28**(12) (1993) 1295–301.
13. Lejeune, M. & Boilot, J. P., Influences of ceramic processing on dielectric properties of perovskite type compound: $\text{Pb}(\text{Mg}_{1/3}\text{Nb}_{2/3})\text{O}_3$. *Ceram. Intl*, **9**(4) (1983) 119–22.
14. Shrout, T. R., Kumar, U., Megheri, M., Yang, N. & Jang, S. J., Grain size dependence and dielectric and electrostriction of $\text{Pb}(\text{Mg}_{1/3}\text{Nb}_{2/3})\text{O}_3$ -based ceramics. *Ferroelectrics*, **76** (1987) 479–87.
15. Wang, H. C. & Schulze, W. A., The role of excess MgO or PbO in determining the microstructure and properties of lead magnesium niobate. *J. Am. Ceram. Soc.*, **73** (1990) 825–32.
16. Okazaki, K., Advanced technology in electroceramics in Japan. *Am. Ceram. Soc. Bull.*, **67**(12) (1988) 1946.
17. Swartz, S. L., Shrout, T. R., Schulze, W. A. & Cross, L. E., Dielectric properties of lead magnesium niobate ceramics. *J. Am. Ceram. Soc.*, **67**(5) (1984) 311–15.
18. Chen, J., Gorton, A., Chen, H. M. & Harmer, M. P., Effect of powder purity and second phase on the dielectric properties of lead magnesium niobate ceramics. *J. Am. Ceram. Soc.*, **69**(12) (1986) C-303–5.
19. ASTM Standard: 1989 *Annual Book of ASTM Standards* Vol. 15.02, C373–88, P109–110. ASTM, Philadelphia, PA., pp. 19103–18.
20. Rushman, D. F. & Strivens, M. A., The effective permittivity of two-phase systems. *Proc. Phys. Soc.*, **59** (1947) 1011–16.
21. Papet, P., Dougherty, J. P. & Shrout, T. R., Particle and grain size effects on the dielectric behavior of the relaxor ferroelectric $\text{Pb}(\text{Mg}_{1/3}\text{Nb}_{2/3})\text{O}_3$. *J. Mater. Res.*, **5** (1990) 2902–9.
22. Viehland, D., Jang, S. J., Wuttig, M. & Cross, L. E., The glassy behaviour of relaxor Ferroelectrics. *Ferroelectrics*, **120** (1991) 71–7.
23. Ackerman, D. A., Moy, D., Potter, R. C., Anderson, A. C. & Lawless, W. N., Glassy behaviour of crystalline solids at low temperature. *Phys. Rev. B*, **23** (1981) 3886–93.
24. Hilton, A., TEM studies of relaxor ferroelectric materials, PhD Thesis, University of Essex, UK (1989).
25. Gupta, S. M., Kulkarni, A. R., Vedpathak, M. & Kulkarni, S. K., Surface study of lead magnesium niobate ceramic using X-ray photoelectron spectroscopy. *J. Mat. Sci. Eng. B* in press.